JCB Article

Identification of a tight junction–associated guanine nucleotide exchange factor that activates Rho and regulates paracellular permeability

Gaëlle Benais-Pont,[1] Anu Punn,[2] Catalina Flores-Maldonado,[3] Judith Eckert,[4] Graça Raposo,[5] Tom P. Fleming,[4] Marcelino Cereijido,[3] Maria S. Balda,[2] and Karl Matter[2]

[1]Department of Cell Biology, University of Geneva, 1211 Geneva, Switzerland
[2]Division of Cell Biology, Institute of Ophthalmology, University College London, EC1V 9EL London, UK
[3]Department of Physiology, Center for Research and Advanced Studies, Mexico, D.F., 07360 Mexico
[4]Division of Cell Sciences, School of Biological Sciences, University of Southampton, SO16 7PX Southampton, UK
[5]Curie Institute, Research Section, Paris 7505, France

Rho family GTPases are important regulators of epithelial tight junctions (TJs); however, little is known about how the GTPases themselves are controlled during TJ assembly and function. We have identified and cloned a canine guanine nucleotide exchange factor (GEF) of the Dbl family of proto-oncogenes that activates Rho and associates with TJs. Based on sequence similarity searches and immunological and functional data, this protein is the canine homologue of human GEF-H1 and mouse Lfc, two previously identified Rho-specific exchange factors known to associate with microtubules in nonpolarized cells. In agreement with these observations, immunofluorescence of proliferating MDCK cells revealed that the endogenous canine GEF-H1/Lfc associates with mitotic spindles. Functional analysis based on overexpression and RNA interference in polarized MDCK cells revealed that this exchange factor for Rho regulates paracellular permeability of small hydrophilic tracers. Although overexpression resulted in increased size-selective paracellular permeability, such cell lines exhibited a normal overall morphology and formed fully assembled TJs as determined by measuring transepithelial resistance and by immunofluorescence and freeze-fracture analysis. These data indicate that GEF-H1/Lfc is a component of TJs and functions in the regulation of epithelial permeability.

Introduction

Epithelial cells interact with each other and with the underlying extracellular matrix using molecular complexes composed of transmembrane proteins and distinct sets of cytoplasmic plaque proteins that serve as connections to the cytoskeleton. These interactions allow epithelial cells to achieve their typical spatial organization and cell surface polarity. Tight junctions (TJs)* are the most apical of the intercellular junctions: they regulate selective paracellular diffusion and restrict the intermixing of apical and basolateral membrane components (Cereijido et al., 2000; Schneeberger and Lynch, 2001). TJ components have also been proposed to be linked to mechanisms that control epithelial polarization and differentiation (Tsukita et al., 1999; Zahraoui et al., 2000; Benais-Pont et al., 2001; Fleming et al., 2001).

TJs are composed of membrane proteins and a cytoplasmic plaque consisting of many different proteins that interact among themselves and interconnect the transmembrane proteins to form large complexes (Cereijido et al., 2000; Tsukita et al., 2001; D'Atri and Citi, 2002). The junctional plaque is formed by different types of proteins that include adapters, such as the ZO proteins, and signaling components, such as small GTPases. The membrane proteins mediate cell adhesion and are thought to constitute the intramembrane and paracellular diffusion barriers. Although it is well known that paracellular diffusion across TJs is size and charge selective and some of the transmembrane proteins have been linked

Address correspondence to Karl Matter, Div. of Cell Biology, Institute of Ophthalmology, University College London, Bath St., London EC1V 9EL, UK. Tel.: 44-20-7608-4014. Fax: 44-20-7608-4034. E-mail: k.matter@ucl.ac.uk; or Maria S. Balda, Div. of Cell Biology, Institute of Ophthalmology, University College London, Bath St., London EC1V 9EL, UK. Tel.: 44-20-7608-4014. Fax: 44-20-7608-4034. E-mail: m.balda@ucl.ac.uk

*Abbreviations used in this paper: cGEF, canine GEF; DH, Dbl homology; GEF, guanine nucleotide exchange factor; PH, pleckstrin homology; TER, transepithelial electrical resistance; TJ, tight junction.

Key words: epithelia; Dbl; intercellular adhesion; actin; microtubules

© The Rockefeller University Press, 0021-9525/2003/03/729/12 $8.00

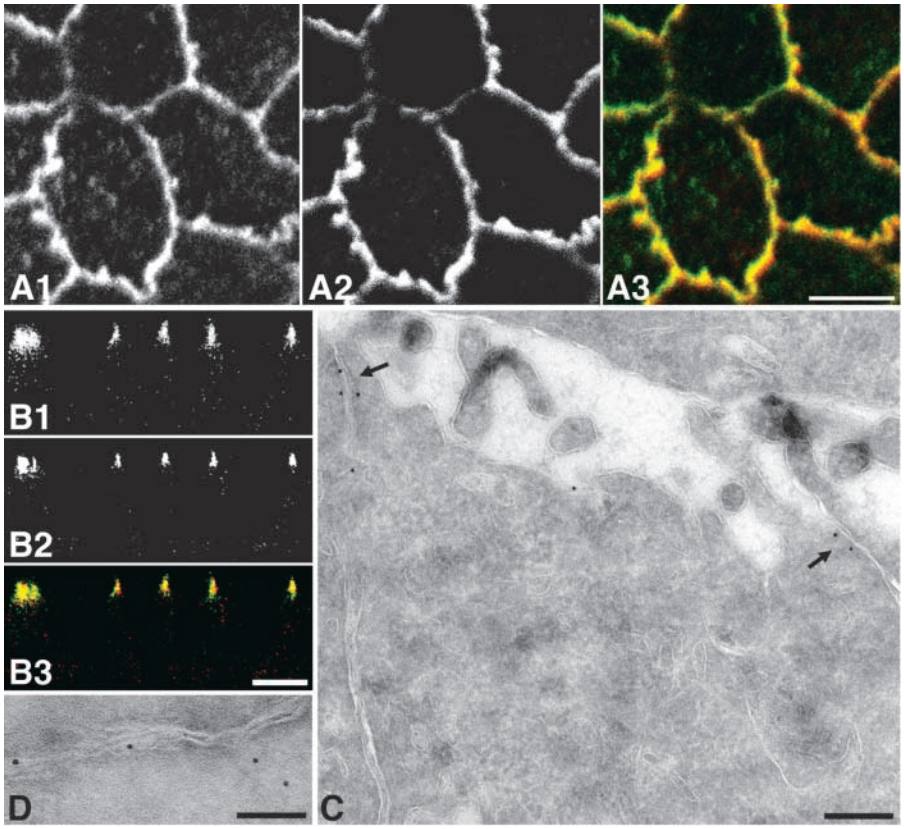

Figure 1. **Subcellular localization of the B4/7 antigen.** (A and B) MDCK cells cultured on polycarbonate filters for 5 d were fixed with methanol and stained with mAb B4/7 (A1 and B1) and polyclonal anti–ZO-1 (A2 and B2) antibodies. Shown are confocal xy (A) and xz (B) sections. A3 and B3 show overlays of the two labelings (B4/7, FITC; anti-ZO-1, Texas red). Bars, 5 μm. (C and D) Ultrathin cryosections of MDCK cells were labeled with B4/7 followed by a rabbit anti–mouse and 5 nm protein A conjugated to colloidal gold (C, apical region of a cell; D, larger magnification of a TJ). The arrows indicate the position of TJs. Bars: (C) 150 nm; (D) 100 nm.

to such processes, the molecular mechanisms responsible for selective paracellular diffusion have not been elucidated but are thought to involve channels or pores embedded into TJ strands (Claude, 1978; Cereijido et al., 1989; Balda and Matter, 2000b; Anderson, 2001; Tsukita et al., 2001).

The actin cytoskeleton plays a crucial role in the regulation of TJs by mechanisms that involve regulation of cortical actin contraction and direct interactions between the actin cytoskeleton and certain TJ components such as occludin, cingulin, and the ZO proteins (Hirokawa and Tilney, 1982; Meza et al., 1982; Madara, 1987; Hecht et al., 1996; Blum et al., 1997; Itoh et al., 1997; Tsukamoto and Nigam, 1997; Turner et al., 1997; Fanning and Anderson, 1998; Cordenonsi et al., 1999; Itoh et al., 1999; Wittchen et al., 1999; Mattagajasingh et al., 2000; Takakuwa et al., 2000; D'Atri and Citi, 2001; Lawrence et al., 2002; Patrie

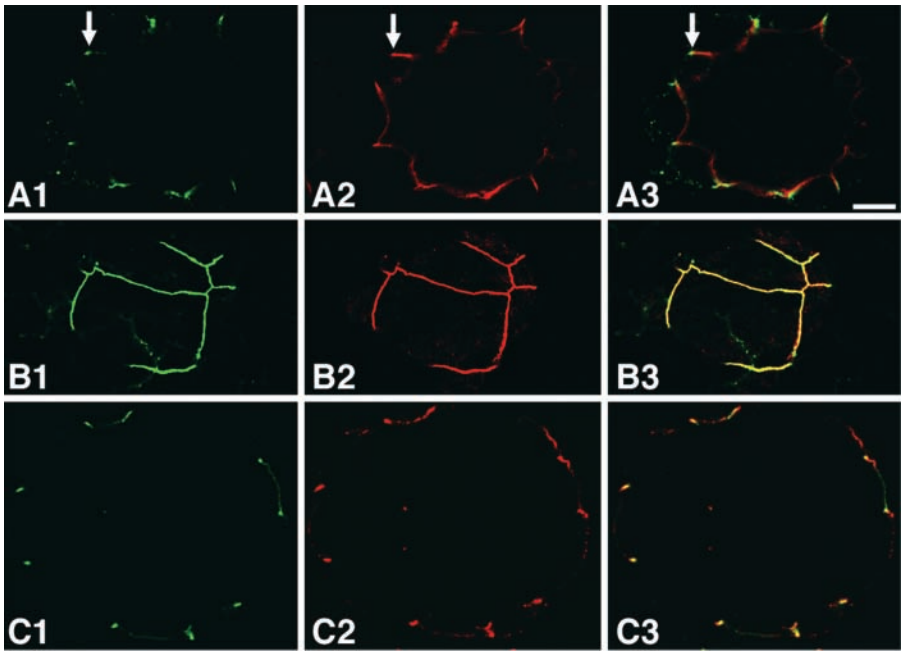

Figure 2. **Immunostaining of the B4/7 antigen in mouse blastocysts.** Embryos were collected and cultured for up to 2 d to the blastocyst stage before removal of the zona pellucida, fixation in 1% formaldehyde, and double staining with mAb B4/7 (A1, B1, and C1) and α-catenin (A2) or ZO-1 (B2 and C2). A3, B, 3 and C3 are overlays of the two labelings. In A and C, midplane optical sections through the trophectoderm wall of the spherical blastocyst are shown, whereas in B, a tangential plane is shown. Arrows in A indicate distinct sites of B4/7 and α-catenin. Bar, 20 μm.

The Journal of Cell Biology

et al., 2002). Rho family GTPases are central regulators of the cytoskeleton (Hall, 1998); consequently, much effort has been put into analyzing their role in TJ assembly and function (Nusrat et al., 1995; Takaishi et al., 1997; Zhong et al., 1997; Jou et al., 1998; Hasegawa et al., 1999; Wojciak-Stothard et al., 2001). Interestingly, the effect of Rho activation on TJs covers a wide spectrum of effects and appears to depend on the extent of activation. For example, overexpression of constitutively active RhoA was shown to cause structural and functional defects (Jou et al., 1998), but Rho stimulation via a transfected prostaglandin receptor resulted in a selective increase in paracellular diffusion of a small molecular weight tracer without a loss of transepithelial electrical resistance (TER) (Hasegawa et al., 1999). Although these studies revealed that Rho and Rac1 regulate TJs, little is known about TJ-related mechanisms that govern activation of these GTPases.

Here we identify a TJ-associated guanine nucleotide exchange factor (GEF) for Rho that associates with the apical junctional complex in cultured and native epithelial cells. The identified canine GEF (cGEF) is the homologue of human GEF-H1 and mouse Lfc, two previously identified Rho GEFs shown to associate with microtubules in transiently transfected nonpolarized cells. Endogenous cGEF-H1 does not bind microtubules in interphase cells but associates with the mitotic spindle during cell division. Using overexpression and RNA interference, we further demonstrate that this GEF functions in the regulation of selective paracellular permeability in MDCK cells. Thus, GEF-H1/Lfc is a functional component of epithelial TJs.

Results

Identification of a TJ-associated Dbl family member

mAb B4/7 stains cell–cell junctions of MDCK cells by immunofluorescence microscopy. Confocal xy and xz sections demonstrated that the B4/7 antigen colocalizes with the TJ marker ZO-1 at the apical end of the lateral membrane, suggesting that it associates with TJs (Fig. 1, A and B). In xz sections, the staining for the B4/7 antigen was slightly less focal than for ZO-1 (Fig. 1, B1 compared with B2). In addition to cell–cell junctions, weak intracellular staining was observed. Immuno-EM of frozen sections confirmed the association of the B4/7 antigen with TJs (Fig. 1, C and D). These observations demonstrate that mAb B4/7 recognizes a TJ-associated protein in MDCK cells. Similar observations were made when the human intestinal epithelial cell line Caco-2 was analyzed (unpublished data).

mAb B4/7 also stains a protein associated with apical intercellular junctions in the trophectoderm of the mouse blastocyst. The antigen was found to localize apical to the adherens junctions identified by α-catenin staining (Fig. 2 A) and to colocalize with the TJ marker ZO-1 (Fig. 2, B and C). In addition to the junctional fluorescence, there was occasionally weak cytoplasmic staining similar to the one seen in MDCK cells. These data suggest that the B4/7 antigen also associates with TJs of a native epithelium.

mAb B4/7 labels a protein of 110 kD in immunoblots of total MDCK cell extracts, which it also immunoprecipitates (Fig. 3 A). We next used the mAb to screen an MDCK expression library, resulting in the isolation of the 3′ end of a partial ORF, which was then completed by rescreening the library with a PCR protocol and finally by 5′ RACE.

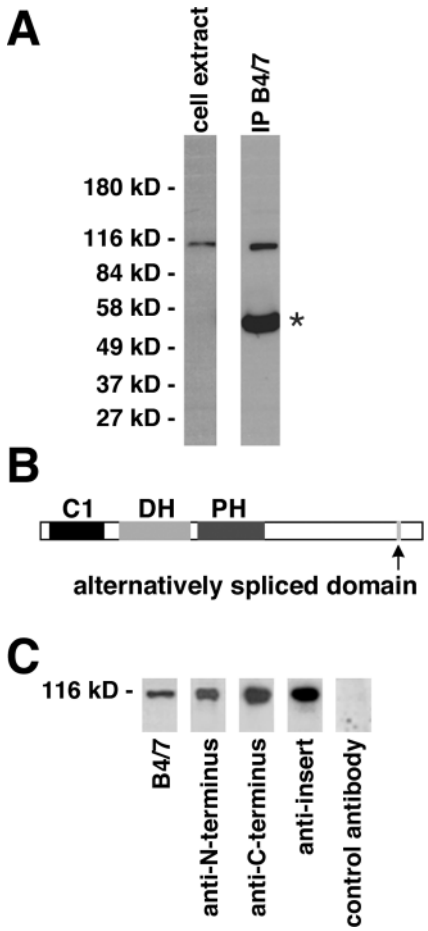

Figure 3. **Molecular identification of the B4/7 antigen.** (A) Total MDCK cell extracts or an immunoprecipitate generated with mAb B4/7 were separated on a 5–15% SDS-PAGE gel and then immunoblotted with B4/7. The asterisk marks the IgG heavy chain. (B) Domain structure of cGEF-H1. Domains identified by PFAM (sequence data available from GenBank/EMBL/DDBJ under accession no. AF494096/AF494097) are shown. (C) B4/7 immunoprecipitates were immunoblotted with antipeptide antibodies generated against both cGEF-H1 termini, the alternative domain, or a control antibody.

Fig. 3 B shows a schematic drawing of the domain structure of the B4/7 antigen. The ORF contains 985 aa with a 22-aa alternatively spliced domain close to the COOH terminus. To verify the cloned sequence, we generated antibodies against peptides representing either one of the termini or the alternatively spliced domain. All three antibodies immunoblotted the 110-kD band immunoprecipitated by mAb B4/7 (Fig. 2 C) and labeled cell–cell junctions by immunofluorescence (see below), confirming that the cloned cDNA indeed represents the B4/7 antigen. By RT-PCR, the isoform containing the insert is the predominant one in MDCK cells (unpublished data). No isoforms in addition to the two variants shown in Fig. 3 B were detected by immunoblotting with the above described antibodies and by RT-PCR of different regions of the cDNA.

Blast and PFAM searches suggested that the cloned protein contains a Dbl homology (DH) and a pleckstrin ho-

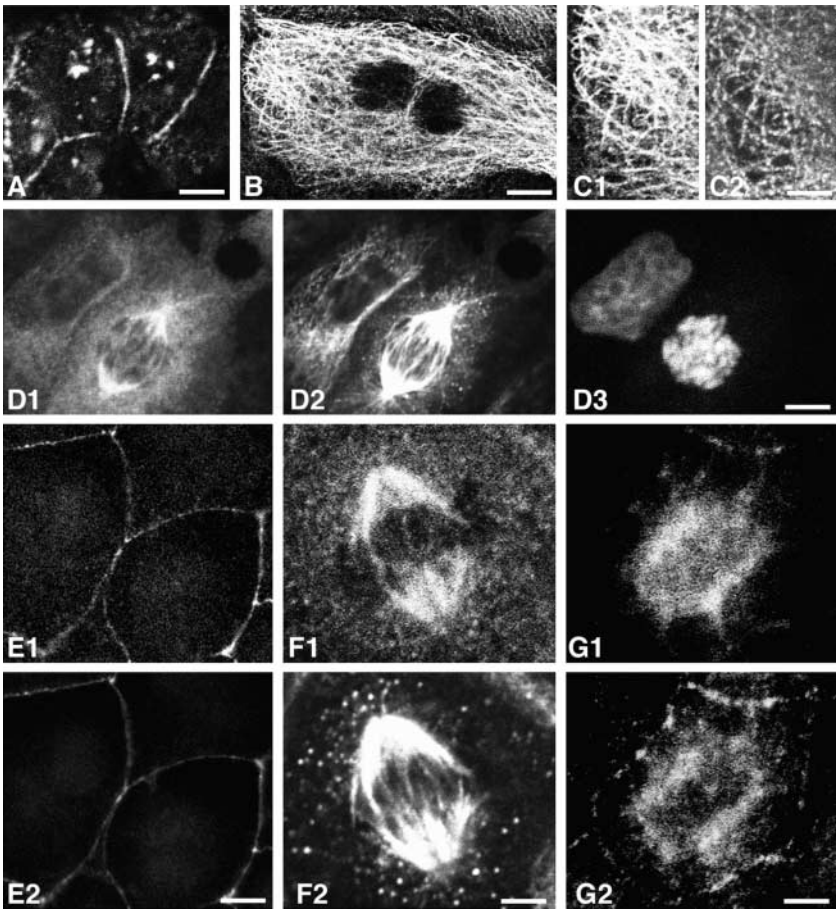

Figure 4. **cGEF-H1 associates with intercellular junctions and microtubules in MDCK cells.** (A) MDCK cells were transiently transfected with HA-tagged cGEF-H1. After 3 d the cells were permeabilized, fixed, and labeled with anti-HA antibodies. Bar, 5 μm. (B and C) Low confluent MDCK cells transiently transfected with HA-cGEF-H1 were fixed with methanol and labeled with anti-HA and anti–α-tubulin antibodies. B shows the anti-HA staining of a strongly expressing cell, and C is a larger magnification of a peripheral region of the cell shown in B (C1, anti-HA; C2, anti–α-tubulin). Bars: (B) 5 μm; (C) 2 μm. (D) Transiently transfected cells were processed as in C. Cells with a moderate expression level (D1, anti-HA; D2, anti–α-tubulin; D3, DNA) are shown. Bar, 5 μm. (E and F) High density wild-type MDCK cells were stained with a peptide antibody against the NH_2 terminus of cGEF-H1 (E1) and an mAb specific for ZO-1 (E2). Bar, 3 μm. (F) Low confluent MDCK cells were stained with antibodies against the NH_2 terminus of cGEF-H1(F1) and anti–α-tubulin (F2). Bar, 3 μm. (G) Low confluent MDCK cells were extracted with Triton X-100 in the presence of Taxol before fixation and then processed for immunofluorescence with mAb B4/7. G1 and G2 show two serial sections of the same cell. Note, a fraction of cGEF-H1 remained associated with junctions during mitosis. Bar, 3 μm.

mology (PH) domain in tandem, a characteristic of the Dbl family of GEFs for Rho GTPases (Whitehead et al., 1997). The searches further predicted an NH_2-terminal C1 domain. The isolated ORF is homologous to two previously identified Dbl family members, mouse Lfc and human GEF-H1, that both possess the same domain structure. An oncogenic variant of mouse Lfc was cloned in a screen for proteins that induces oncogenic transformation and functions as a GEF for Rho (Whitehead et al., 1995; Glaven et al., 1996). Human GEF-H1 has the same domain structure and is known to activate Rho (Ren et al., 1998; Krendel et al., 2002).

Both GEF-H1 and Lfc had originally been identified as smaller proteins that lacked much of the domain COOH-terminal to the PH domain. However, Krendel et al. (2002) recently described a longer version of GEF-H1 (sequence data available from GenBank/EMBL/DDBJ under accession no. AF486838) that is >90% identical to the here described canine protein. A homologous sequence of identical length of mouse Lfc (sequence data available from GenBank/EMBL/DDBJ under accession no. AF177032) has been deposited in GenBank. Since several of the earlier reported truncated sequences were cloned from transformed cells and/or were identified because of their transforming potential, the truncated forms appear to represent oncogenic variants. Human GEF-H1 and mouse Lfc have previously been concluded to represent homologues (Krendel et al., 2002). Since the high degree of similarity suggested that the three proteins represent homologues, we used Blast searches of the human genome to test whether they map to the same locus. These searches revealed that the cloned canine sequence and mouse Lfc have the highest homology to the gene of GEF-H1 on human chromosome 1. Similarly, all three proteins mapped to the same locus when the mouse genome was searched. Because of these homologies and the experiments described below, we concluded that the three GEFs indeed represent homologues; hence, we call the here cloned the protein cGEF-H1.

Localization of GEF-H1 to the actin cytoskeleton and microtubules

Tagged versions of Lfc and GEF-H1 were demonstrated to associate with microtubules in nonpolarized cells (Ren et al., 1998; Glaven et al., 1999; Krendel et al., 2002). To determine whether this is also the case for the cloned cGEF, we constructed cDNAs with an NH_2-terminal HA epitope (HA-cGEF-H1). Fig. 4 A shows that HA-cGEF-H1 was found at cell–cell junctions in transiently transfected MDCK cells at low expression levels. Additionally, there was some cytoplasmic fluorescence that became stronger with increasing expression. Non-tagged cGEF-H1 was localizing more efficiently to TJs (see below), suggesting that the tag interferes with normal localization. We could not detect a difference in localization between constructs with and without the alternatively spliced domain (unpublished data). However, at high expression levels HA-cGEF-H1 was found to associate with filaments (Fig. 4 B). These filaments were labeled with anti–α-tubulin antibodies, indicating that they

The Journal of Cell Biology

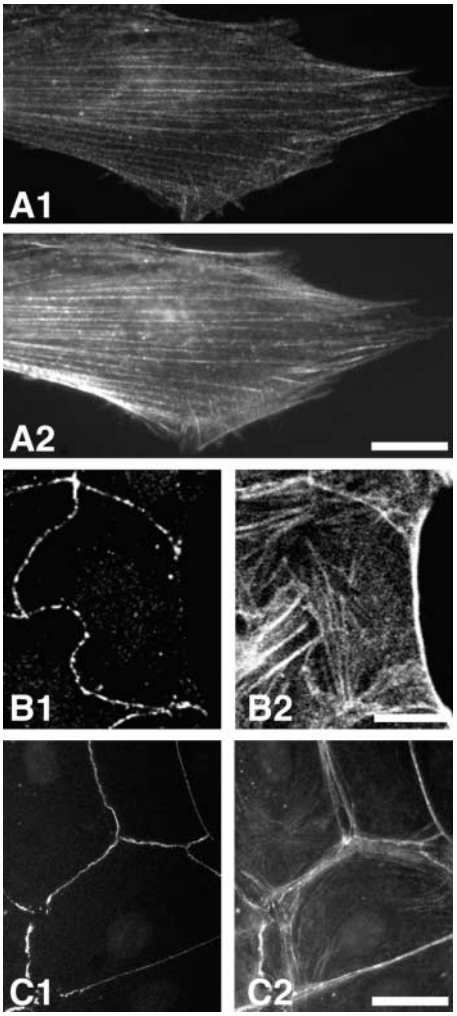

Figure 5. **cGEF-H1 associates with different actin-based cytoskeletal structures in different cell types.** Low confluent MRC-5 fibroblasts (A), MDCK (B), and Caco-2 (C) cells were fixed with PFA, permeabilized with Triton X-100, and fluorescently labeled with B4/7 (A1, B1, and C1) and TRITC-phalloidin (A2, B2, and C2). Bars, 6 μm.

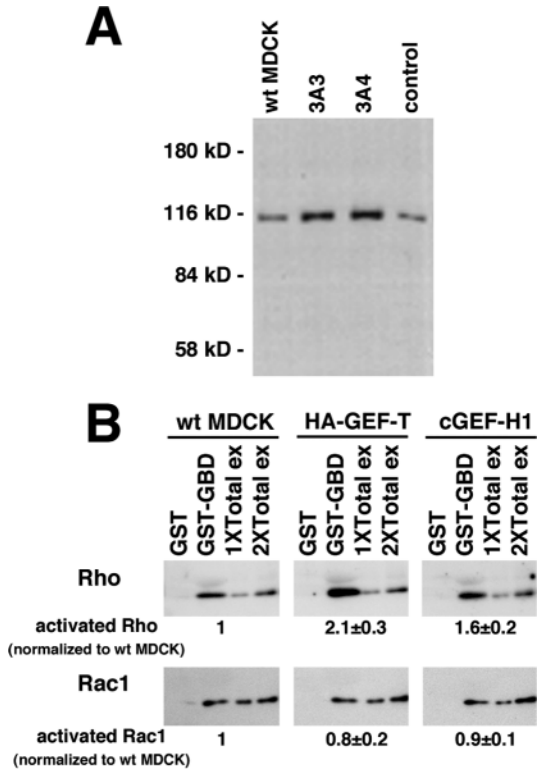

Figure 6. **Activation of Rho by cGEF-H1.** (A) Total cell extracts of wild-type (wt) or transfected MDCK cells were immunoblotted with mAb B4/7. 3A3 and 3A4, clones overexpressing cGEF-H1; control, clone derived from control transfection. (B) Wild-type and transfected MDCK cells expressing truncated cGEF-H1 (HA-GEF-T) or wild-type cGEF-H1 were extracted and tested for the presence of activated Rho or Rac1 by performing pull-down assays with recombinant fusion proteins lacking (GST) or containing a GTPase-binding domains of (GST-GBD). The pulled-down fractions were analyzed by immunoblotting for the presence of Rho or Rac1. Increasing amounts of total cell extracts were loaded on the gels to normalize the amount of GTPases in different cell extracts (1X Total ex and 2X Total ex). Immunoblots were quantified by densitometric scanning, and the values obtained for the activated GTPase were divided by those obtained in total cell extracts. All ratios were then normalized to wild-type cells and expressed as fold activation (mean ± SD of three experiments; both increases in active Rho are significant, $p < 0.05$ using the Student's *t* test).

are microtubules (Fig. 4 C). Fig. 4 D shows that clear microtubule association was not observed at low expression levels in interphase cells but was pronounced in mitotic cells in which the transfected protein was found at the mitotic spindle. Thus, transfected epitope-tagged cGEF-H1 can associate with microtubules similar to human GEF-H1 and mouse Lfc.

Given these observations, it was surprising that endogenous cGEF-H1 was associated with TJs in interphase cells since microtubules are not detected close to intercellular junctions. Additionally, the distribution of endogenous cGEF-H1 was not affected by the depolymerization of microtubules with nocodazole, indicating that the junctional association does not depend on microtubules (unpublished data). Nevertheless, the above described observations suggest that cGEF-H1 may associate with microtubules under certain conditions such as mitosis. To test this, we used the above described antibodies to test whether endogenous GEF-H1 can be detected at the mitotic spindle. Fig. 4 E shows that the antibody generated against the NH_2 terminus labeled TJs in wild-type MDCK cells. However, in mitotic cells GEF-H1 was found to concentrate at the mitotic spindle (Fig. 4 F). Similar observations were made with the antibodies specific for the COOH terminus and the alternatively spliced domain (unpublished data). mAb B4/7 stained the mitotic spindle inefficiently and only after Triton X-100 extraction, suggesting that the epitope recognized by the mAb is blocked when cGEF-H1 is associated with microtubules (Fig. 4 G). Junctional GEF staining in mitotic cells often appeared heterogeneous, which might be caused by the recruitment of a fraction of junctional cGEF-H1 to mitotic spindles. These data indicate that endogenous cGEF-H1 is concentrated at TJs in interphase cells but also associates with spindle microtubules during mitosis.

We next used the human fibroblast cell line MRC-5 to test whether association of endogenous GEF-H1 with non-

The Journal of Cell Biology

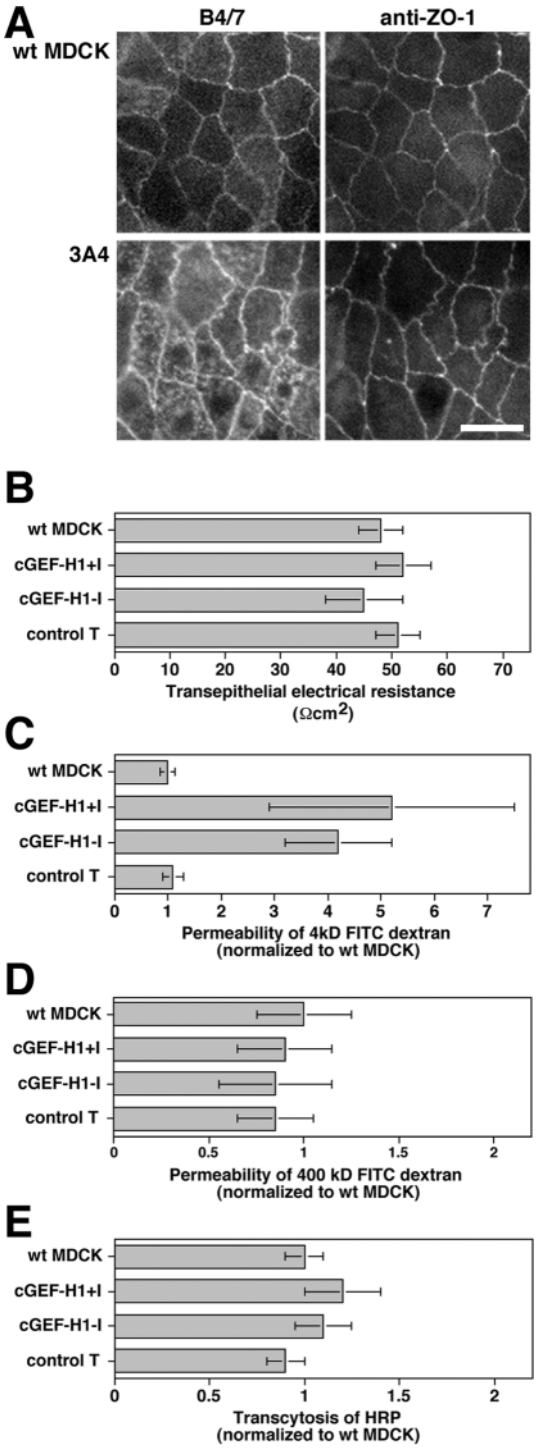

Figure 7. **Functional analysis of TJs of cells overexpressing cGEF-H1.** (A) Wild-type (wt) and cGEF-H1–overexpressing (3A4) cells, cultured for 1 wk on polycarbonate filters, were fixed and processed for double immunofluorescence using mAb B4/7 and anti–ZO-1 antibodies. Images obtained with constant microscope sensitivity settings are shown. Bar, 10 μm. (B and C) MDCK cells were cultured on filters for 1 wk and were then analyzed first by measuring TER (B) and, after a time of recovery, by determining paracellular permeability of 4 kD FITC-dextran (C) or 400 kD FITC-dextran (D). At the end, the cultures were analyzed for overexpression of cGEF-H1 by immunoblotting (examples are shown in Fig. 3 A). All values of transfected cells represent means ± SD of several independent clones: four clones were analyzed for cGEF-H1+I, three clones for cGEF-H1-I, and three control clones that were derived from a transfection of the empty vector. The increases in 4 kD FITC-dextran permeability of overexpressing cells are significant (cGEF-H1+I, $p < 0.02$ and cGEF-H1-I, $p < 0.05$ using the Student's *t* test) (E) Fluid phase transcytosis was measured after labeling cells for 10 min at 37°C with HRP from the apical side. Cells were then cooled on ice and extensively washed. Transcytosis was then allowed to proceed for 2 h at 37°C. Basolateral media were then collected, and transcytosed HRP was measured. Averages obtained from two different clones for each type of transfection are shown.

microtubule-based structures can also be observed in nonpolarized cells. Fig. 5 A shows that endogenous GEF-H1 was found to associate with filaments that were stained with phalloidin, indicating that they are actin filaments. Interestingly, stress fibers were not stained by anti–GEF-H1 antibodies in low confluent MDCK cells but the labeling coincided with the F-actin staining at cell–cell junctions (Fig. 5 B). Similarly, endogenous GEF-H1 colocalized with F-actin at cell–cell junctions and not at stress fibers in the human intestinal epithelial cell line Caco-2 (Fig. 5 C). This suggests that GEF-H1 can localize to different types of actin-based structures in different cell types.

Overexpression of cGEF-H1 results in Rho activation

Human GEF-H1 and mouse Lfc function as activators of Rho (Glaven et al., 1996; Krendel et al., 2002). To test whether cGEF-H1 indeed functions as a GEF for Rho, we generated cell lines overexpressing either wild-type cGEF-H1 (Fig. 6 A) or an HA-tagged truncated mutant containing only the DH and PH domains, a type of mutation that results in constitutively active variants of Dbl family members. Activation of Rho was then tested by performing pull-down assays with GST fusion proteins containing the GTPase-binding domain of rhotekin; in control experiments, αPAK was used to pull down Rac1 as a control, since this GTPase is not activated by GEF-H1/Lfc (Glaven et al., 1996; Benard et al., 1999; Ren et al., 1999; Nakagawa et al., 2001; Krendel et al., 2002).

Fig. 6 B shows that overexpression of truncated GEF-H1 (HA-GEF-T) resulted in a more than twofold up-regulation of active Rho, whereas the levels of active Rac were not affected. The transfected truncated protein accumulated in the cytosol and expression was paralleled by a large increase in stress fibers and cell spreading (unpublished data), further supporting Rho activation. Overexpression of full-length cGEF-H1 resulted in an increase in active Rho by >50%, and no changes in the levels of active Rac1 were detected. Overexpression of wild-type cGEF-H1 did not cause an obvious change in the actin cytoskeleton such as an increase in stress fibers (unpublished data), suggesting that Rho activation by the wild-type GEF was spatially more restricted to TJs.

GEF-H1 regulates paracellular permeability of MDCK cell monolayers

We next tested whether overexpression of cGEF-H1 affects TJ functions. Since we have thus far not been able to generate epitope-tagged proteins that accumulate efficiently at TJs at high expression levels, we used stable cell lines such as those shown in Fig. 6 A that overexpress wild-type cGEF-

The Journal of Cell Biology

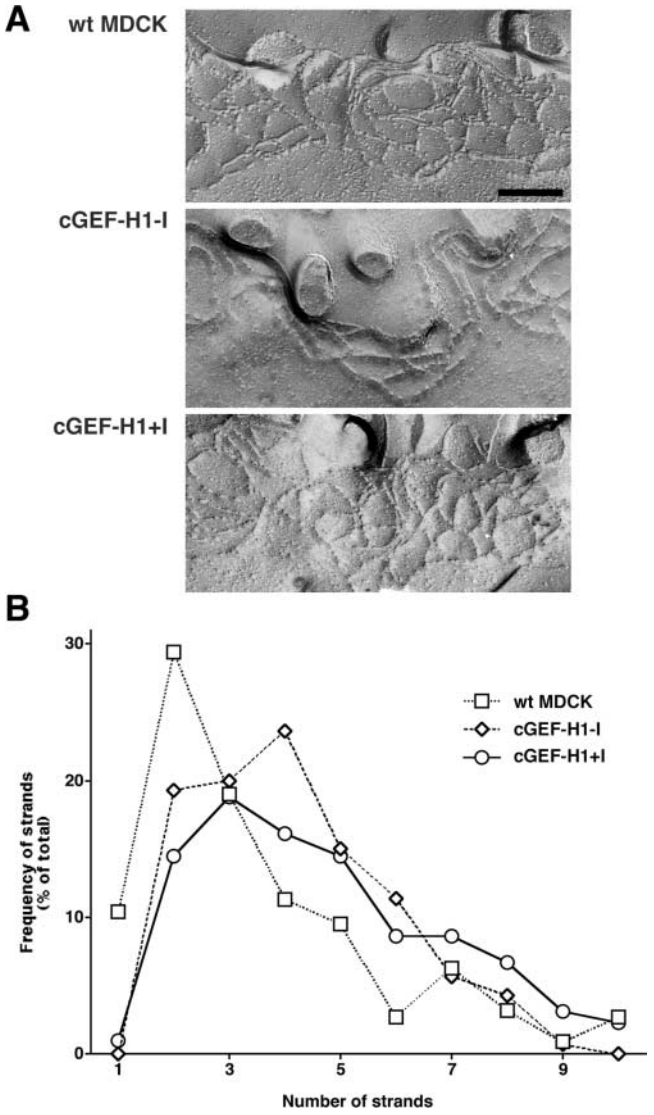

Figure 8. **Freeze-fracture analysis of TJs.** (A) MDCK cells were fixed and processed for freeze-fracture. Images of wild-type cells and cells overexpressing cGEF-H1-I and cGEF-H1+I, respectively, are shown. Bar, 150 nm. (B). Images obtained from freeze-fracture replicas were quantified over a total distance of 44.2 μm for wild-type cells, 28.0 μm for cGEF-H1-I, and 50.8 μm for cGEF-H1+I–overexpressing cells. The total number of segments counted for each cell line was set to 100%.

H1 at least fivefold to avoid artifacts induced by the epitope tags. Immunofluorescence of filter-grown cells demonstrated that overexpressed cGEF-H1 accumulated efficiently at TJs and that the cells formed apparently normal monolayers (Fig. 7 A). At the immunofluorescence level, neither the distribution of ZO-1 (Fig. 7 A) nor of the transmembrane proteins occludin and claudin-4 (unpublished data) was affected by cGEF-H1 overexpression. Furthermore, staining with fluorescent phalloidin did not reveal changes in the distribution of F-actin (unpublished data).

To determine whether cGEF-H1–overexpressing cells still formed electrically tight monolayers, we measured TER. Fig. 7 B shows that TER was not altered by cGEF-H1 overexpression, supporting the conclusion that monolayer formation was not affected. In contrast, paracellular permeability of 4 kD FITC-dextran was found to be four- to fivefold up-regulated in cells overexpressing either one of the two identified isoforms (Fig. 7 C). Similar results were obtained when permeability of tritiated mannitol was measured (unpublished data). In contrast, paracellular permeability of 400 kD FITC-dextran was not affected, indicating that the increase was specific for small molecular weight tracers (Fig. 7 D). Overexpression of cGEF-H1 did not affect transcytosis of HRP, indicating that the increase in 4 kD FITC-dextran permeability was not due to increased fluid phase transcytosis (Fig. 7 E). These data suggest that cGEF-H1 functions in the regulation of paracellular permeability.

In freeze-fracture replicas, TJs appear as a characteristic network of intramembrane strands. The integrity of this network is generally taken as evidence for correct assembly of TJs. Therefore, we next analyzed the appearance of TJs in wild-type and cGEF-H1–overexpressing cells by freeze-fracture. Fig. 8 A shows that overexpression did not inhibit the formation of intramembrane strands. Quantification of the number of strands revealed that overexpression of neither of the two isoforms resulted in a reduction of the number of strands (Fig. 8 B). This further supports the conclusion that overexpression of cGEF-H1 did not result in increased paracellular permeability because of a defect in TJ assembly.

To test the relevance of endogenous cGEF-H1 in the regulation of paracellular permeability, we used RNA interference to reduce expression of the endogenous protein. Stable cell lines were generated that expressed short RNA duplexes directed against either one of two different regions of cGEF-H1 (GEF-RD-I and GEF-RD-II). Expression was then compared with cells transfected with a plasmid driving the expression of a control RNA duplex with a random sequence (control-RD). Immunoblotting demonstrated that expression of cGEF-H1 could be significantly reduced by expression of either one of the two cGEF-H1–directed RNA duplexes (Fig. 9 A), and immunofluorescence with mAb B4/7 revealed that both junctional and cytoplasmic fluorescence were reduced (Fig. 9 B).

We next analyzed the effects of reduced expression of cGEF-H1 on TJ functions. Fig. 9 C shows that TER was not affected by the reduced expression of cGEF-H1. In contrast, paracellular permeability of 4 kD FITC-dextran was reduced by ~50% in cells expressing cGEF-H1–directed RNA duplexes in comparison to wild-type MDCK cells and control transfections (Fig. 9 D). These data further support the conclusion that cGEF-H1 functions in the regulation of paracellular permeability.

Discussion

RhoA is an important regulator of TJ, but regulators of Rho that localize to TJs have not been identified previously. Here, we describe the identification of a Dbl family member as a novel functional component of TJs that associates with this intercellular junction in cultured and native epithelia. This junctional GEF is the canine homologue of human GEF-H1 and mouse Lfc. This protein activates Rho and regulates paracellular permeability of small hydrophilic trac-

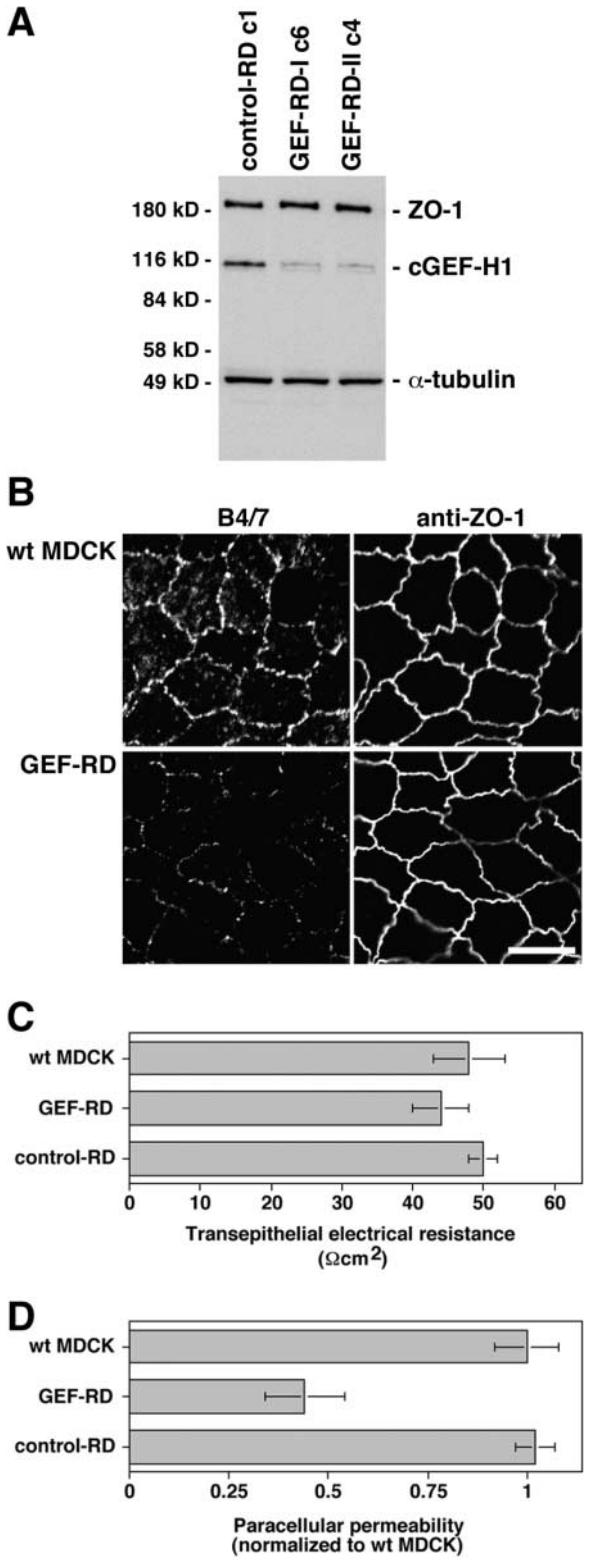

Figure 9. **Analysis of MDCK cells with reduced expression of GEF-H1.** (A) MDCK cells transfected with a plasmid driving the expression of a control RNA duplex (control-RD c1) or RNA duplex targeting different regions of cGEF-H1 (GEF-RD-I c6 and GEF-RD-II c4) were harvested, and expression was analyzed by immunoblotting with mAb B4/7. ZO-1 and α-tubulin were immunoblotted as controls. The reduction of GEF-H1 expression in all clones used for the functional analysis was at least 50%. (B–D) MDCK cells were cultured on filters for 9 d and were then analyzed by immunofluorescence (B shows labelings with mAb B4/7 and a polyclonal anti–ZO-1 antibody; Bar, 8 μm), by measuring TER (C), and by determining paracellular permeability of 4 kD FITC-dextran (D). The values represent means ± SD of four clones for cells with reduced cGEF-H1 expression (GEF-RD) and two clones for control transfections (control-RD). The decrease in paracellular permeability of GEF-RD cells is significant ($p < 0.01$ using the Student's *t* test).

ers. Increased permeability was not associated with a breakdown of the junctional barrier as determined morphologically and by measuring TER and permeability of a high molecular weight tracer. Given the importance of Rho in the regulation of paracellular permeability (Hecht et al., 1996; Turner et al., 1997; Fujita et al., 2000; Hirase et al., 2001), this suggests that this TJ-associated GEF is part of a Rho-based permeability-regulating pathway.

Identification of cGEF-H1

Molecular cloning of the antigen recognized by mAb B4/7 resulted in the isolation of a canine cDNA that is >90% identical with human GEF-H1 and its mouse homologue Lfc, which share a similar degree of homology with each other, suggesting that we have isolated the canine homologue of GEF-H1/Lfc. This is supported by the observation that the three proteins match best to the same gene in the human and the mouse genome. Furthermore, transfected epitope-tagged cGEF-H1 accumulates at microtubules, which was also observed for human GEF-H1 and mouse Lfc. Additionally, antipeptide antibodies against sequences that are identical in the three GEFs recognize TJs in canine and human epithelial cells.

It was surprising to find a protein known to associate with microtubules on TJs, which are linked to the actin cytoskeleton and not microtubules (Hirokawa and Tilney, 1982; Meza et al., 1982; Madara, 1987; Fanning, 2001). However, immunofluorescence in different cell types indicated that endogenous GEF-H1 can localize to different actin-based structures such as the TJs in epithelial cells and stress fibers in a fibroblast cell line. Moreover, endogenous GEF-H1 was found to concentrate at mitotic spindles, indicating that GEF-H1 can associate with both the actin cytoskeleton and microtubules.

We have not observed a clear microtubule staining (with antibodies that were raised against sequences identical in canine and human GEF-H1 and mouse Lfc) in nontransfected interphase cells using several epithelial and nonepithelial cell lines (e.g., MDCK, Caco-2, HeLa, MRC-5, and 3T3). In low confluent cells, we observed fine intracellular dots that occasionally aligned along microtubules (unpublished data). However, the significance of this observation is not clear, since only a fraction of these dots were close to microtubules. Since our antibodies are able to detect GEF-H1 on mitotic spindles, the absence of microtubule staining in interphase cells is unlikely to be due to problems with epitope accessibility but may rather reflect a yet to be identified regulatory mechanism that controls the differential subcellular localization of GEF-H1 in interphase and mitotic cells. Since GEF-H1 is a phosphoprotein and its phosphorylation depends on the proliferation state in MDCK cells (unpublished data), it could be that localization of GEF-H1 is regulated by protein phosphorylation.

The Journal of Cell Biology

GEF-H1 and the regulation of paracellular permeability

Increased permeability by cGEF-H1 overexpression did not result in a disruption of TJ strands, suggesting that cGEF-H1 overexpression activated a mechanism that either regulates or mediates selective paracellular permeability (Balda and Matter, 2000b; Cereijido et al., 2000; Tsukita et al., 2001). Given our limited understanding of the mechanisms mediating selective paracellular permeability, it is not clear whether this involves modifications of the junctional actin cytoskeleton or changes in the activities of components of TJ strands such as claudins or occludin.

Activation of Rho has been linked previously to regulation of TJ structure and function (Nusrat et al., 1995; Takaishi et al., 1997; Zhong et al., 1997; Jou et al., 1998; Hasegawa et al., 1999; Hirase et al., 2001; Wojciak-Stothard et al., 2001). Although overexpression of constitutively active or dominant-negative RhoA was shown to result in striking morphological alterations, such as a loss of the normal TJ strand morphology (Jou et al., 1998), activation of endogenous Rho was linked to selective functional changes without obvious effects on TJ structure. Hasegawa et al. (1999) demonstrated that activation of Rho in MDCK cells via a transfected prostaglandin receptor results in a selective increase in paracellular permeability of small molecular weight tracers. It will be interesting to test whether cGEF-H1 becomes activated by this prostaglandin receptor. However, since prostaglandin treatment was paralleled by increased TER, although in our study TER was not affected by increases or decreases in cGEF-H1 expression, these two proteins may be part of different regulatory pathways. Alternatively, prostaglandin receptors may activate more than one pathway: one regulating paracellular permeability and another one ion conductivity.

Regulation of TJs by Rho is likely to involve different pathways and varies with the cell type analyzed. Several studies linked the Rho effector ROCKI to the regulation of TJ assembly and paracellular permeability. This pathway is thought to modify TJs by regulating myosin phosphorylation and hence contraction of the cortical actin cytoskeleton. Depending on the conditions and/or cell type analyzed, activation of ROCKI was linked to TJ assembly and increases in TER or to junction disassembly and increased permeability (Gopalakrishnan et al., 1998; Fujita et al., 2000; Hirase et al., 2001; Walsh et al., 2001; Wojciak-Stothard et al., 2001). In our experiments, treatment with the ROCKI inhibitor Y27632 resulted in a loss of the paracellular barrier (unpublished data). Given these observations, it is possible that integrity of TJs and regulation of paracellular permeability requires a balance between different Rho effector pathways. This is supported by the recent observation that ROCKI and DiaI represent opposing Rho effector pathways that regulate adherens junction formation and dynamics (Sahai and Marshall, 2002). Additionally, different stimuli that cause activation of Rho can result in increases in endothelial permeability via a ROCKI-dependent or -independent pathway, suggesting that at least two different Rho pathways regulate paracellular permeability (Hirase et al., 2001).

Possible additional functions of GEF-H1

In addition to paracellular permeability, GEF-H1 may be involved in other Rho-regulated processes. For example, GEF-H1 may participate in events that require rearrangements of intercellular junctions. In endothelia, leukocyte transmigration requires Rho activation (Adamson et al., 1999). Therefore, GEF-H1 may become activated during transmigration to stimulate the required cytoskeletal rearrangements.

It has been demonstrated recently that apoptotic cells are extruded by their neighbors in MDCK monolayers (Rosenblatt et al., 2001). This process requires stimulation of Rho and contraction of the cortical actin cytoskeleton. Although it is not know how apoptotic cells signal to their neighbors, it could be that this involves activation of Rho by the TJ-associated GEF-H1.

In addition to regulating processes occurring at TJ, cGEF-H1 may also function in the regulation of epithelial cell proliferation and differentiation. RhoA and Rac1 are regulated in opposite ways: Rac1 is up-regulated and RhoA down-regulated when cells reach full confluence and assemble cell–cell junctions, whereas Ras transformation causes Rac1 inactivation and RhoA activation (Zondag et al., 2000; Fukata and Kaibuchi, 2001). Hence, TJs may help to control RhoA activity by recruiting cGEF-H1 to TJs in mature monolayers and, in the absence of a stimulus, inactivating its GEF activity.

Since GEF-H1 associates with the mitotic spindle, it could be that it participates in the regulation of cell division. Cytokinesis is a Rho-dependent process, suggesting that GEF-H1 could be important to complete the cell cycle (Glotzer, 2001). Strikingly, microtubule-associated GEF-H1 becomes activated when microtubules are depolymerized by nocodazole in transfected cells (Krendel et al., 2002). Hence, it could be that depolymerization of spindle microtubules during cytokinesis activates GEF-H1, and subsequently Rho, resulting in cytokinesis and assembly of intercellular junctions between the two daughter cells.

These are interesting possible functions for GEF-H1, and their study may lead to the identification of novel mechanisms by which TJs can participate in the regulation of diverse cellular functions. It will also be important to identify interacting proteins in order to understand how GEF-H1 can associate with microtubules and the actin cytoskeleton and how these processes are regulated. Moreover, the association with stress fibers in fibroblasts, but TJs in epithelial cells suggests that different interacting proteins may function as linkers to the actin cytoskeleton in different cell types. Information about interacting partners may ultimately also help us to understand how GEF-H1 becomes activated in different subcellular locations and triggers activation of Rho.

Materials and methods

Antibodies

mAb B4/7 was derived from a mouse immunized with a protein fraction isolated from detergent extracts of MDCK cells using fusion proteins containing the cytoplasmic domain of low density lipoprotein receptor. Binding of GEF-H1 to this fusion protein was not specific. Hybridoma production and subcloning were as described (Hauri et al., 1985). Five subclones of the originally isolated hybridoma line were isolated and found to recognize all the same protein in immunoblots and to produce the same pattern in immunofluorescence experiments.

All peptides and antipeptide antibodies were produced by Gramsch Laboratories. The following peptides were used to generate rabbit polyclonal antibodies: anti–cGEF-H1 NH_2 terminus, MSRIESLTRARTERC; anti–

The Journal of Cell Biology

cGEF-H1 COOH terminus, CDFTRMQDIPEETES; anti–cGEF-H1 alternative domain, CRGHDRLDLSVTIRSVH; anti–ZO-1, YTDQELDETLNDEVC; and anti–claudin-4, PRTDKPYSAKYSAAC. The peptides were conjugated to epoxy-activated Sepharose (Amersham Biosciences), and the antibodies were affinity purified as described (Balda et al., 1996). For α-tubulin, mAb 1A2 was used (Kreis, 1987), and in some immunofluorescence experiments ZO-1 was detected with rat monoclonal R40.76 (Anderson et al., 1988) or with a rabbit polyclonal antibody (Sheth et al., 1997). α-Catenin was detected with the M12K rabbit polyclonal antibody (Herrenknecht et al., 1991). GTPases were detected by immunoblotting using the following anti-GTPase antibodies: Rho, rabbit polyclonal antibody sc-179 anti-RhoA (Santa Cruz Biotechnology, Inc.) and Rac1, mouse mAb 102 (BD Transduction Laboratories).

Cloning of canine GEF-H1/Lfc and generation of stable cell lines

mAb B4/7 was used to screen pTEX-based MDCK expression libraries (Herz et al., 1990; Balda and Matter, 2000a). The 5′ end was cloned by PCR screening (Takumi and Lodish, 1994) and 5′ RACE (FirstChoice™ RLM RACE kit; Ambion). For sequence analysis and homology searches, we used ClustalW, Pfam, and the Blast search of the Ensembl Genome Browser with the human genome database.

The cDNAs coding for the full-length protein with or without the alternative domain were then assembled in the cytomegalovirus-based expression vector pCB6 for stable expression. HA-tagged truncated GEF-H1 (HA-GEF-T) containing the DH and the PH domain was generated by PCR and cloned into pCB6 containing the HA epitope (Balda et al., 1996). Stably transfected MDCK cell lines were generated as described previously (Balda et al., 1996).

The mU6pro vector was used for the expression of RNA duplexes (Yu et al., 2002). Two regions of canine GEF-H1 were targeted that are part of sequences coding for different protein domains (region I, 5′-AACAAGAGCATCACAGCCAAG-3′ and region II, 5′-AATGTGACTATCCACAACCGC-3′). Derivatives of the mU6pro vector were constructed as described (Yu et al., 2002) and cotransfected with a plasmid carrying a puromycin resistance gene for the selection of stable cell lines.

Several clones were analyzed for each type of transfection: three clones for cGEF-H1 with the alternatively spliced domain, three clones for cGEF-H1 lacking the alternatively spliced domain, three control clones that were derived from a transfection of the empty vector, four clones expressing cGEF-H1–directed RNA duplexes, and two clones expressing control RNA duplexes with a random sequence.

Analysis of TJ functions, transcytosis, pull-down assays, and immunoblots

Wild-type and transfected MDCK cells were plated on 12-well Transwell Filters and cultured for at least 7 d before the paracellular permeability measurements (Balda et al., 1996). After this time of culture, all transfected cell lines exhibited stable TER values that did not significantly change anymore from one day to the other. TER and paracellular flux of FITC-dextran (4 and 400 kD) were measured as described (Balda et al., 1996).

To measure fluid–phase transcytosis, cells grown on filters were allowed to take up HRP (10 mg/ml) for 10 min at 37°C. Internalization was stopped by cooling the cells on ice, and the cells were then washed six times for 3 min with cold PBS containing 0.5% BSA. The cultures were incubated again at 37°C for 120 min, and the media were collected and transcytosed HRP was measured with a colorimetric assay (Matter et al., 1994).

Plasmids for GST fusion proteins containing GTPase-binding domains were produced as described (Ren et al., 1999; Nakagawa et al., 2001). Fusion proteins were stored at –80°C for a maximum of 2 wk. For pull-down assays, cells were grown in 15-cm tissue culture plates. Cells were extracted, and active GTPases were pulled down as described (Ren et al., 1999; Nakagawa et al., 2001). Immunoblotting was done as described previously using HRP-conjugated secondary antibodies and the ECL chemiluminescence detection system (Amersham Biosciences).

Microscopy

For immunofluorescence, the cultured cells were either fixed with methanol at –20°C without preextraction or permeabilized and fixed with Triton X-100 and 3% PFA (Balda et al., 1996). Filter-grown cells were fixed and permeabilized with ethanol/acetone or with methanol at –20°C (Balda et al., 1996). To stain mitotic spindles with mAb B4/7, cells were extracted with 0.2% Triton X-100 in 100 mM KCl, 3 mM $MgCl_2$, 1 mM $CaCl_2$, 200 mM sucrose, and 10 mM Hepes (pH 7.1) on ice in the presence of 10 μM Taxol before fixation with methanol. The samples were incubated with antibodies and mounted as described previously (Balda et al., 2000). DNA was stained with TO-PRO-3 (Molecular Probes). Fluorescent secondary antibodies were obtained from Molecular Probes or Jackson ImmunoResearch Laboratories, Inc.

For immunolocalization experiments in mouse blastocysts, preimplantation embryos were collected from superovulated and mated MF1 female mice and cultured in T6 medium with BSA to the blastocyst stage as described previously (Sheth et al., 2000). Embryos, after removal of the zona pellucida, were fixed in 1% formaldehyde for 10 min and permeabilized in 0.25% Triton X-100 before antibody incubations in specialized chambers (Sheth et al., 2000). Secondary antibodies conjugated to fluorescent Alexa dyes were from Cambridge Bioscience. Embryos were examined whole mount.

For immuno-EM, MDCK cells were fixed with 3% PFA and then processed for cryosectioning and immunolabeling (Liou et al., 1996; Raposo et al., 1997). Freeze-fracture analysis was performed as described previously (Balda et al., 1996). The morphometric analysis was performed on micrographs of freeze-fracture replicas that were printed at 50,000× magnification. Lines parallel to the main axis of the TJ were traced, and series of perpendicular lines were then drawn (one line every 200 nm). The number of strands of a given segment of TJs was defined as the number of its intersections with the perpendicular line.

We thank Drs. M.A. Schwartz (The Scripps Research Institute, La Jolla, CA) and K. Kaibuchi (Nagoya University, Aichi, Japan) for reagents, Dr. P. Frankel for advice on the GTPase pull-down assay, and Dr. S. M. Moss for critical reading of the manuscript.

This research was supported by Cancer Research UK (SP2562/0101–2632), The Wellcome Trust (063661 and 066100), Fight for Sight, and the Swiss National Science Foundation.

Submitted: 12 November 2002
Revised: 16 January 2003
Accepted: 16 January 2003

References

Adamson, P., S. Etienne, P.O. Couraud, V. Calder, and J. Greenwood. 1999. Lymphocyte migration through brain endothelial cell monolayers involves signaling through endothelial ICAM-1 via a rho-dependent pathway. *J. Immunol.* 162:2964–2973.

Anderson, J.M. 2001. Molecular structure of tight junctions and their role in epithelial transport. *News Physiol. Sci.* 16:126–130.

Anderson, J.M., B.R. Stevenson, L.A. Jesaitis, D.A. Goodenough, and M.S. Mooseker. 1988. Characterization of ZO-1, a protein component of the tight junction from mouse liver and Madin-Darby canine kidney cells. *J. Cell Biol.* 106:1141–1149.

Balda, M.S., and K. Matter. 2000a. The tight junction protein ZO-1 and an interacting transcription factor regulate ErbB-2 expression. *EMBO J.* 19:2024–2033.

Balda, M.S., and K. Matter. 2000b. Transmembrane proteins of tight junctions. *Semin. Cell Dev. Biol.* 11:281–289.

Balda, M.S., J.A. Whitney, C. Flores, S. González, M. Cereijido, and K. Matter. 1996. Functional dissociation of paracellular permeability and transepithelial electrical resistance and disruption of the apical-basolateral intramembrane diffusion barrier by expression of a mutant tight junction membrane protein. *J. Cell Biol.* 134:1031–1049.

Balda, M.S., C. Flores-Maldonado, M. Cereijido, and K. Matter. 2000. Multiple domains of occludin are involved in the regulation of paracellular permeability. *J. Cell. Biochem.* 78:85–96.

Benais-Pont, G., K. Matter, and M.S. Balda. 2001. Intracellular signaling in classical and new tight junction functions. *In* Tight Junctions. J.M. Anderson and M. Cereijido, editors. CRC Press, Boca Roton, FL. 367–394.

Benard, V., B.P. Bohl, and G.M. Bokoch. 1999. Characterization of rac and cdc42 activation in chemoattractant-stimulated human neutrophils using a novel assay for active GTPases. *J. Biol. Chem.* 274:13198–13204.

Blum, M.S., E. Toninelli, J.M. Anderson, M.S. Balda, J. Zhou, L. O'Donnell, R. Pardi, and J.R. Bender. 1997. Cytoskeletal rearrangement mediates human microvascular endothelial tight junction modulation by cytokines. *Am. J. Physiol.* 273:H286–H294.

Cereijido, M., L. González-Mariscal, and G. Contreras. 1989. Tight junction: barrier between higher organisms and environment. *News Physiol. Sci.* 4:72–74.

Cereijido, M., L. Shoshani, and R.G. Contreras. 2000. Molecular physiology and pathophysiology of tight junctions. I. Biogenesis of tight junctions and epithelial polarity. *Am. J. Physiol. Gastrointest. Liver Physiol.* 279:G477–G482.

Claude, P. 1978. Morphological factors influencing transepithelial permeability: a

model for the resistance of the zonula occludens. *J. Membr. Biol.* 39:219–232.
Cordenonsi, M., F. D'Atri, E. Hammar, D.A. Parry, J. Kendrick-Jones, D. Shore, and S. Citi. 1999. Cingulin contains globular and coiled-coil domains and interacts with ZO-1, ZO-2, ZO-3, and myosin. *J. Cell Biol.* 147:1569–1582.
D'Atri, F., and S. Citi. 2001. Cingulin interacts with F-actin in vitro. *FEBS Lett.* 507:21–24.
D'Atri, F., and S. Citi. 2002. Molecular complexity of vertebrate tight junctions. *Mol. Membr. Biol.* 19:103–112.
Fanning, A.S. 2001. Organization and the regulation of the tight junction by the actin-myosin cytoskeleton. *In* Tight Junctions. J.M. Anderson and M. Cereijido, editors. CRC Press, Boca Roton, FL. 265–284.
Fanning, A.S., and J.M. Anderson. 1998. The tight junction protein ZO-1 establishes a link between the membrane protein occludin and the actin cytoskeleton. *J. Biol. Chem.* 273:29745–29753.
Fleming, T.P., B. Sheth, and I. Fesenko. 2001. Cell adhesion in the preimplantation mammalian embryo and its role in trophectoderm differentiation and blastocyst morphogenesis. *Front. Biosci.* 6:D1000–D1007.
Fujita, H., H. Katoh, H. Hasegawa, H. Yasui, J. Aoki, Y. Yamaguchi, and M. Negishi. 2000. Molecular decipherment of Rho effector pathways regulating tight-junction permeability. *Biochem. J.* 346:617–622.
Fukata, M., and K. Kaibuchi. 2001. Rho-family GTPases in cadherin-mediated cell-cell adhesion. *Nat. Rev. Mol. Cell Biol.* 2:887–897.
Glaven, J.A., I.P. Whitehead, T. Nomanbhoy, R. Kay, and R.A. Cerione. 1996. Lfc and Lsc oncoproteins represent two new guanine nucleotide exchange factors for the Rho GTP-binding protein. *J. Biol. Chem.* 271:27374–27381.
Glaven, J.A., I. Whitehead, S. Bagrodia, R. Kay, and R.A. Cerione. 1999. The Dbl-related protein, Lfc, localizes to microtubules and mediates the activation of Rac signaling pathways in cells. *J. Biol. Chem.* 274:2279–2285.
Glotzer, M. 2001. Animal cell cytokinesis. *Annu. Rev. Cell Dev. Biol.* 17:351–381.
Gopalakrishnan, S., N. Raman, S.J. Atkinson, and J.A. Marrs. 1998. Rho GTPase signaling regulates tight junction assembly and protects tight junctions during ATP depletion. *Am. J. Physiol.* 275:C798–C809.
Hall, A. 1998. Rho GTPases and the actin cytoskeleton. *Science.* 279:509–514.
Hasegawa, H., H. Fujita, H. Katoh, J. Aoki, K. Nakamura, A. Ichikawa, and M. Negishi. 1999. Opposite regulation of transepithelial electrical resistance and paracellular permeability by Rho in Madin-Darby canine kidney cells. *J. Biol. Chem.* 274:20982–20988.
Hauri, H.-P., E.E. Sterchi, D. Bienz, J.A.M. Fransen, and A. Marxer. 1985. Expression and intracellular transport of microvillus membrane hydrolases in human intestinal epithelial cells. *J. Cell Biol.* 101:838–851.
Hecht, G., L. Pestic, G. Nikcevic, A. Koutsouris, J. Tripuraneni, D.D. Lorimer, G. Nowak, V. Guerriero, Jr., E.L. Elson, and P.D. Lanerolle. 1996. Expression of the catalytic domain of myosin light chain kinase increases paracellular permeability. *Am. J. Physiol.* 271:C1678–C1684.
Herrenknecht, K., M. Ozawa, C. Eckerskorn, F. Lottspeich, M. Lenter, and R. Kemler. 1991. The uvomorulin-anchorage protein alpha catenin is a vinculin homologue. *Proc. Natl. Acad. Sci. USA.* 88:9156–9160.
Herz, J., N. Flint, K. Stanley, R. Frank, and B. Dobberstein. 1990. The 68 kDa protein of signal recognition particle contains a glycine-rich region also found in certain RNA-binding proteins. *FEBS Lett.* 276:103–107.
Hirase, T., S. Kwashima, E.Y. Wong, T. Ueyama, Y. Rikitake, S. Tsukita, M. Yokoyama, and J.M. Staddon. 2001. Regulation of tight junction permeability and occludin phosphorylation by RhoA-p160ROCK-dependent and -independent mechanisms. *J. Biol. Chem.* 276:10423–10431.
Hirokawa, N., and L.G. Tilney. 1982. Interactions between actin filaments and between actin filaments and membranes in quick-frozen and deeply etched hair cells of the chick ear. *J. Cell Biol.* 95:249–261.
Itoh, M., A. Nagafuchi, S. Moroi, and S. Tsukita. 1997. Involvement of ZO-1 in cadherin-based cell adhesion through its direct binding to alpha catenin and actin filaments. *J. Cell Biol.* 138:181–192.
Itoh, M., K. Morita, and S. Tsukita. 1999. Characterization of ZO-2 as a MAGUK family member associated with tight as well as adherens junctions with a binding affinity to occludin and alpha catenin. *J. Biol. Chem.* 274:5981–5986.
Jou, T.S., E.E. Schneeberger, and W.J. Nelson. 1998. Structural and functional regulation of tight junctions by RhoA and Rac1 small GTPases. *J. Cell Biol.* 142:101–115.
Kreis, T.E. 1987. Microtubules containing detyrosinated tubulin are less dynamic. *EMBO J.* 6:2597–2606.
Krendel, M., F.T. Zenke, and G.M. Bokoch. 2002. Nucleotide exchange factor GEF-H1 mediates cross-talk between microtubules and the actin cytoskeleton. *Nat. Cell Biol.* 4:294–301.
Lawrence, D.W., K.M. Comerford, and S.P. Colgan. 2002. Role of VASP in reestablishment of epithelial tight junction assembly after Ca2+ switch. *Am. J. Physiol. Cell Physiol.* 282:C1235–C1245.
Liou, W., H.J. Geuze, and J.W. Slot. 1996. Improving structural integrity of cryosections for immunogold labeling. *Histochem. Cell Biol.* 106:41–58.
Madara, J.L. 1987. Intestinal absorptive cell tight junctions are linked to cytoskeleton. *Am. J. Physiol.* 253:C171–C175.
Mattagajasingh, S.N., S.-H. Huang, J.S. Hartenstein, and E.J. Benz. 2000. Characterization of the interaction between protein 4.1R and ZO-2: a possible link between the tight junction and the actin cytoskeleton. *J. Biol. Chem.* 275:30573–30585.
Matter, K., E.M. Yamamoto, and I. Mellman. 1994. Structural requirements and sequence motifs for polarized sorting and endocytosis of LDL and Fc receptors in MDCK cells. *J. Cell Biol.* 126:991–1004.
Meza, I., M. Sabanero, E. Stefani, and M. Cereijido. 1982. Occluding junctions in MDCK cells: modulation of transepithelial permeability by the cytoskeleton. *J. Cell. Biochem.* 18:407–421.
Nakagawa, M., M. Fukata, M. Yamaga, N. Itoh, and K. Kaibuchi. 2001. Recruitment and activation of Rac1 by the formation of E-cadherin-mediated cell-cell adhesion sites. *J. Cell Sci.* 114:1829–1838.
Nusrat, A., M. Giry, J.R. Turner, S.P. Colgan, C.A. Parkos, D. Carnes, E. Lemichez, P. Boquet, and J.L. Madara. 1995. Rho protein regulates tight junctions and perijunctional actin organization in polarized epithelia. *Proc. Natl. Acad. Sci. USA.* 92:10629–10633.
Patrie, K.M., A.J. Drescher, A. Welihinda, P. Mundel, and B. Margolis. 2002. Interaction of two actin-binding proteins, synaptopodin and alpha-actinin-4, with the tight junction protein MAGI-1. *J. Biol. Chem.* 277:30183–30190.
Raposo, G., M.J. Kleijmeer, G. Posthuma, J.W. Slot, and H.J. Geuze. 1997. Immunogold labeling of ultrathin cryosections: application in immunology. *Handbook Exp. Immunol.* 4:1–11.
Ren, X.D., W.B. Kiosses, and M.A. Schwartz. 1999. Regulation of the small GTP-binding protein Rho by cell adhesion and the cytoskeleton. *EMBO J.* 18:578–585.
Ren, Y., R. Li, Y. Zheng, and H. Busch. 1998. Cloning and characterization of GEF-H1, a microtubule-associated guanine nucleotide exchange factor for Rac and Rho GTPases. *J. Biol. Chem.* 273:34954–34960.
Rosenblatt, J., M.C. Raff, and L.P. Cramer. 2001. An epithelial cell destined for apoptosis signals its neighbors to extrude it by an actin- and myosin-dependent mechanism. *Curr. Biol.* 11:1847–1857.
Sahai, E., and C.J. Marshall. 2002. ROCK and Dia have opposing effects on adherens junctions downstream of Rho. *Nat. Cell Biol.* 4:408–415.
Schneeberger, E.E., and R.D. Lynch. 2001. Ultrastructure and immuno-labeling of the tight junction. *In* Tight Junctions. J.M. Anderson and M. Cereijido, editors. CRC Press, Boca Roton, FL. 19–37.
Sheth, B., I. Fesenko, J.E. Collins, B. Moran, A.E. Wild, J.M. Anderson, and T.P. Fleming. 1997. Tight junction assembly during mouse blastocyst formation is regulated by late expression of ZO-1 alpha+ isoform. *Development.* 124:2027–2037.
Sheth, B., B. Moran, J.M. Anderson, and T.P. Fleming. 2000. Post-translational control of occludin membrane assembly in mouse trophectoderm: a mechanism to regulate timing of tight junction biogenesis and blastocyst formation. *Development.* 127:831–840.
Takaishi, K., T. Sasaki, H. Kotani, H. Nishioka, and Y. Takai. 1997. Regulation of cell-cell adhesion by rac and rho small G proteins in MDCK cells. *J. Cell Biol.* 139:1047–1059.
Takakuwa, R., Y. Kokai, T. Kojima, T. Akatsuka, H. Tobioka, N. Sawada, and M. Mori. 2000. Uncoupling of gate and fence functions of MDCK cells by the actin-depolymerizing reagent mycalolide B. *Exp. Cell Res.* 257:238–244.
Takumi, T., and H.F. Lodish. 1994. Rapid cDNA cloning by PCR screening. *Biotechniques.* 17:443–444.
Tsukamoto, T., and S.K. Nigam. 1997. Tight junction proteins form large complexes and associate with the cytoskeleton in an ATP depletion model for reversible junction assembly. *J. Biol. Chem.* 272:16133–16139.
Tsukita, S., M. Furuse, and M. Itoh. 1999. Structural and signalling molecules come together at tight junctions. *Curr. Opin. Cell Biol.* 11:628–633.
Tsukita, S., M. Furuse, and M. Itoh. 2001. Multifunctional strands in tight junctions. *Nat. Rev. Mol. Cell Biol.* 2:285–293.
Turner, J.R., B.K. Rill, S.L. Carlson, D. Carnes, R. Kerner, R.J. Mrsny, and J.L. Madara. 1997. Physiological regulation of epithelial tight junctions is associated with myosin light-chain phosphorylation. *Am. J. Physiol.* 273:C1378–C1385.
Walsh, S.V., A.M. Hopkins, J. Chen, S. Narumiya, C.A. Parkos, and A. Nusrat. 2001.

The Journal of Cell Biology

Rho kinase regulates tight junction function and is necessary for tight junction assembly in polarized intestinal epithelia. *Gastroenterology.* 121:566–579.

Whitehead, I., H. Kirk, C. Tognon, G. Trigo-Gonzalez, and R. Kay. 1995. Expression cloning of lfc, a novel oncogene with structural similarities to guanine nucleotide exchange factors and to the regulatory region of protein kinase C. *J. Biol. Chem.* 270:18388–18395.

Whitehead, I.P., S. Campbell, K.L. Rossman, and C.J. Der. 1997. Dbl family proteins. *Biochim. Biophys. Acta.* 1332:F1–F23.

Wittchen, E.S., J. Haskins, and B.R. Stevenson. 1999. Protein interactions at the tight junction. Actin has multiple binding partners, and ZO-1 forms independent complexes with ZO-2 and ZO-3. *J. Biol. Chem.* 274:35179–35185.

Wojciak-Stothard, B., S. Potempa, T. Eichholtz, and A.J. Ridley. 2001. Rho and Rac but not Cdc42 regulate endothelial cell permeability. *J. Cell Sci.* 114: 1343–1355.

Yu, J.Y., S.L. DeRuiter, and D.L. Turner. 2002. RNA interference by expression of short-interfering RNAs and hairpin RNAs in mammalian cells. *Proc. Natl. Acad. Sci. USA.* 99:6047–6052.

Zahraoui, A., D. Louvard, and T. Galli. 2000. Tight junction, a platform for trafficking and signaling protein complexes. *J. Cell Biol.* 151:F31–F36.

Zhong, C., M.S. Kinch, and K. Burridge. 1997. Rho-stimulated contractility contributes to the fibroblastic phenotype of Ras-transformed epithelial cells. *Mol. Biol. Cell.* 8:2329–2344.

Zondag, G.C., E.E. Evers, J.P. ten Klooster, L. Janssen, R.A. van der Kammen, and J.G. Collard. 2000. Oncogenic Ras downregulates Rac activity, which leads to increased Rho activity and epithelial-mesenchymal transition. *J. Cell Biol.* 149:775–782.

The Journal of Cell Biology